

A Comparative Electron-Spin-Resonance Study of the Ground State and a Photoconverted Metastable State of the Mg^+ Donor in Silicon*

J. E. Baxter and G. Ascarelli

Physics Department, Purdue University, Lafayette, Indiana 47907

(Received 17 July 1972)

Magnesium diffused into silicon forms a deep-double-donor state. Depending on the compensation, the distinct valence states Mg^0 , Mg^+ , or Mg^{++} are possible. EPR measurements have been performed at 55 GHz on the paramagnetic valence state Mg^+ at liquid-helium temperatures. In thermal equilibrium, with the sample in the dark, the EPR absorption of Mg^+ is consistent with the Mg^+ ion occupying the tetrahedral interstitial position, with $1s(A_1)$ as the electronic ground state. This confirms previous optical-absorption work. With near-infrared light incident on the sample ($1 \lesssim \lambda \lesssim 2 \mu$), this paramagnetic center is converted to a metastable state $(Mg^+)^*$, where the Mg^+ ion is displaced from T_d to an interstitial position along the $\langle 111 \rangle$ axis of the Si unit cell. Although only a small g shift of Mg^+ results from such a conversion, large changes are observed in both the contact interaction with the magnesium nucleus and the spin-lattice relaxation time. The optical conversion is total below $\sim 14^\circ K$, where the characteristic lifetime is of the order of minutes. In the dark, $(Mg^+)^*$ decays back to $(Mg^+; T_d)$ with second-order kinetics. This optical conversion can be explained either by an ionic-motion model or by an electron transfer process involving Mg^{++} ions associated with a substitutional lattice defect.

I. INTRODUCTION

Impurity states in semiconductors, most notably in silicon and germanium, are one of the most extensively studied topics in solid-state physics. Group-III and group-V impurities in Si and Ge have been successfully treated by the effective-mass approximation¹ (EMA). The appropriate model for these defects is the hydrogen atom, with the Coulomb potential reduced by $1/\epsilon_s$ because of the electrostatic shielding of the surrounding crystalline environment (characterized by the static dielectric constant ϵ_s). Since the resulting binding energy is small, the electron orbits are large. The appropriate electron mass is then the effective mass of the relevant energy band of the host crystal.

The validity of the EMA has been established by the observation of the hydrogenic optical excitation spectrum² of group-III acceptors and group-V donors in Si and Ge. The complexity of both the valence and conduction bands modifies, in a calculable way, the simplest hydrogenic spectrum that would result in an isotropic medium. Such band complexities have been directly observed in cyclotron-resonance experiments.³

For donors in silicon, each hydrogenic state is sixfold degenerate because of the six equivalent $\langle 100 \rangle$ conduction-band (CB) minima. Although the agreement between the calculated and observed spectra is good for the p states, the ground-state agreement is poor, i.e., different binding energies are observed among the group-V donors. It is necessary, therefore, to include contributions arising from the core electrons of a particular donor to the binding energy of the valence electron in order to explain this discrepancy. Because of the

tetrahedral field at the donor site, the sixfold degenerate $1s$ ground state is split into $1s(A_1)$, $1s(E)$, and $1s(T_2)$. The separation between these states depends on the interaction of the loosely bound valence electron with the remaining electrons of the donor. The singlet $1s(A_1)$ generally has an energy which is lower than either the doublet $1s(E)$ or the triplet $1s(T_2)$. The singlet wave function is an equally weighted linear combination of $1s$ states localized under the six equivalent CB minima of Si; it gives a nonvanishing value for $|\psi(0)|^2$, and thus the "chemical shift" of this state is the largest. The doublet and triplet states have $|\psi(0)|^2 = 0$ and lie near the EMA binding energy. In thermal equilibrium at low temperatures, only $1s(A_1)$ is populated and thus probed by EPR.

The variety of information that can be obtained by EPR studies of donor states is best illustrated by the work of Feher,⁴ dealing with the group-V donors in Si. The chemical shift of these impurities is relatively small; they are termed "shallow." Impurities which form deeper states, with binding energies considerably larger than the EMA value (~ 30 MeV), are less well understood. The primary example of a deep donor has been sulphur, whose substitutional nature has been indicated by optical⁵ and EPR⁶ work. Impurities can also enter the silicon lattice as interstitials, an example being lithium.^{7,8} This shallow donor exhibits a near degeneracy of $1s(A_1)$, $1s(E)$, and $1s(T_2)$ (very small chemical shift) not found for any other donor. Iron-group transition metals in silicon have also been studied.⁹ They can form deep-donor states at either substitutional or interstitial lattice positions. Their study, as well as that of sulfur and lithium, has been complicated by their tendency towards

association, either with themselves or with compensating donors and acceptors. The formation of such complexes has been clearly established by EPR.⁹

Magnesium in silicon^{10,11} is of interest because it is a double donor, like sulfur, and an interstitial, like lithium. Since magnesium has two valence electrons, it is the solid-state analog of the helium atom. Optical-absorption studies^{10,11} on magnesium-doped silicon have established the interstitial nature of this impurity because of the observed donorlike excitation spectrum. The lighter group-II element beryllium, on the other hand, gives an acceptorlike excitation spectrum¹² and is thus believed to be substitutional. The spectrum arising from the allowed $1s \rightarrow np$ transitions of neutral magnesium donors differs from those of the group-V donors by a constant energy arising from the larger binding of the former. Singly ionized magnesium has a separation between the different np states roughly four times those of Mg^0 . The delocalized np states of magnesium can thus be described rather well by the EMA. The position of the $1s$ ground state does not agree with what would be expected from scaling the atomic results for helium, where the binding energies of Mg^0 and Mg^+ would be expected to be ~ 55 MeV (He atom) and $4 \times 30 \approx 120$ MeV (He^+), respectively.¹¹ The experimental values are significantly larger,^{11,13} 107.5 meV for Mg^0 and 256.5 meV for Mg^+ . Magnesium in silicon is thus a "deep" donor.

The atomic configuration of Mg^+ is $[Ne] 3s^1$. In view of the odd number of electrons, Mg^+ is expected to be paramagnetic and a candidate for EPR. By contrast since Mg^0 contains an even number of electrons, it is not expected to be paramagnetic. Experimentally, EPR absorption has only been observed by us in silicon containing Mg^+ . Only this valence state will be discussed in this paper. The present EPR work on Mg^+ was initiated to verify the result of optical experiments¹¹ that the Mg^+ ion occupies the tetrahedral (T_d) interstitial position with $1s(A_1)$ as its electronic ground state. The measured EPR parameters can then be compared, along with the previous optical data, to future chemical-shift calculations for this interstitial deep donor. Our EPR work does confirm the T_d symmetry and the $1s(A_1)$ electronic assignment. Electron-nuclear double resonance (ENDOR)^{4,14} would provide a more detailed study of the $1s(A_1)$ state of Mg^+ ; it can distinguish the T_d substitutional from the T_d interstitial lattice sites. ENDOR measurements do not appear to be feasible, however, because of the very low Mg^+ concentrations ($\sim 10^{14} \text{ cm}^{-3}$). The ENDOR requirement of a long spin-lattice relaxation time T_1 is however easily satisfied at liquid-helium temperatures (LHeT). In addition to an EPR study of ($Mg^+ : T_d$), another species of Mg^+ has been detected

when the Si samples were illuminated with near-infrared light. A report on the study of this state, ($Mg^+)^*$, and its relation to ($Mg^+ : T_d$) is another purpose of this paper. Possible models for the photoconversion of ($Mg^+ : T_d$), and its subsequent recovery, will be proposed in Sec. IV.

II. EXPERIMENTAL PROCEDURE

Singly ionized magnesium can be created either by thermal ionization of neutral magnesium donors¹⁰ ($T \gtrsim 90^\circ \text{K}$), or by diffusing magnesium into silicon containing group-III acceptors.¹³ This valence state can be made to coexist with Mg^0 by electron bombardment at room temperature of intrinsic silicon into which magnesium has been previously diffused.¹³ Our EPR samples were prepared by diffusing pure magnesium¹⁵ into floating-zone silicon doped with $\sim 10^{15}$ boron acceptors/ cm^3 in a manner described by Ho and Ramdas.¹¹ Following diffusion near 1150°C (for about 8 h), the samples were dropped into liquid nitrogen. Such a rapid thermal quench is necessary to avoid the precipitation of the low-solubility magnesium. The quenched samples were prepared to have a thin-circular-disk geometry, whose 8-mm diameter was that of a cylindrical TE_{01n} microwave cavity. For a typical disk thickness of 1.15 mm, the samples had a magnetic filling factor of ~ 0.3 . Such large filling factors are necessary to perform EPR on samples containing $\sim 10^{14} \text{ Mg}^+$ ions/ cm^3 .

In addition to using natural magnesium [which contains 10% of the Mg^{25} isotope (nuclear spin $\frac{5}{2}$)], samples were prepared from magnesium enriched¹⁶ to contain 99.2% Mg^{25} . Such isotropically enriched samples serve to distinguish the Mg^+ EPR absorption from other paramagnetic defects found in our thermally quenched samples. Such an identification is possible from the $(2I+1)$ -hyperfine-line "signature" provided by (Mg^{25})⁺ donors. EPR spectra assigned to Fe^0 , Fe^+ , Cr^0 , and Cr^+ were also detected. Their identification is based on a comparison with the spectra reported in Ref. 9. A light-sensitive center believed to be related to the compensating boron acceptors has also been detected¹⁷ below 6°K . Above this temperature the linewidths become too large to yield an observable EPR. Such a broadening may be due to a rapid decrease in the spin-lattice relaxation time with increasing temperature.^{9,18}

The low solubility of magnesium in silicon yields a concentration gradient that is easily apparent by comparing the EPR intensities of a sample with first one face, and then the other, placed on the cavity wall where the microwave magnetic field is a maximum. Such intensity differences were most pronounced in samples where Mg was diffused from only one side. Density gradients are also indicated by the fact that the experimentally determined "av-

erage" Mg^+ densities are typically $2 \times 10^{14} \text{ cm}^{-3}$, while the compensating boron has a uniform density of $1.5 \times 10^{15} \text{ cm}^{-3}$; only Mg^{2+} would be expected in such a uniformly doped sample. With our sample preparation experience, most of the Mg^+ donors occupy the region $\leq 0.3 \text{ mm}$ from the surface. Another problem with this impurity is its long-term instability. A gradual decrease in concentration takes place over a period of months^{11,13,17}; such an instability would be expected for an interstitial impurity.⁹

A 55-GHz superheterodyne microwave spectrometer with a 65-kG superconducting solenoid was used in our experiments. The details can be found elsewhere.¹⁷ The minimum detectable spin density at 4.2 °K with this system was $\sim 10^{11} \text{ spins/cm}^3$ G, for an incident power level of 1 μW . This figure was determined from EPR measurements on phosphorus-doped silicon (filling factor, 0.2). The relatively high frequency of our spectrometer is necessary to resolve the small g shift of $(\text{Mg}^+)^*$ in relation to $(\text{Mg}^+ : T_d)$. The solenoid had a 1.5-in. bore, allowing ample room for cavity design at 20 kG ($g \sim 2$).

Variable-temperature operation was provided by surrounding the cavity with helium exchange gas and by using a nonmagnetic heater wire wound around the cavity body. A $\frac{1}{10}$ -W carbon resistor mounted on the cavity served as a thermometer. The cavity resonant frequency could be varied $\pm 0.5 \text{ GHz}$ by changing the penetration depth of a fused-quartz finger protruding into the cavity. This tuning finger was the tapered tip of a quartz light pipe, by means of which the sample was illuminated. The Si (Mg^+) samples were cut so as to have either the $\langle 111 \rangle$ or the $\langle 110 \rangle$ cubic axis parallel to the magnetic field. Cyclotron resonance was used to check the orientation of the Si (Mg^+) samples *in situ*, by taking advantage of the well-known¹⁹ mass anisotropy of conduction-band electrons.

The g values and hyperfine splittings, spin densities, and the spin-lattice relaxation times for both species of Mg^+ were measured simultaneously with those corresponding to a phosphorus-doped silicon standard sample, mounted in the cavity with the Si (Mg^+) samples. This technique provides a direct comparison of the spectrum of a deep donor with that of an extensively studied shallow donor whose EPR parameters have been accurately measured.^{4,20} This comparison is independent of instrumental effects. It also provides for a direct relative-impurity-concentration measurement and avoids calibration problems (hysteresis effects) with the solenoid.

III. EXPERIMENTAL RESULTS AND DISCUSSION

A. Thermal Equilibrium State $(\text{Mg}^+ : T_d)$

Ho and Ramdas,¹¹ as a result of their piezospectroscopic measurements, have assigned the Mg^+

ion to the tetrahedral interstitial position, with the singlet as the ground state. The spin Hamiltonian for $(\text{Mg}^{25})^*$ donors should then be the same form as that found for the group-V donors⁴:

$$\mathcal{H} = g\mu_B \vec{S} \cdot \vec{H} + A_D \vec{I}_D \cdot \vec{S} + \left(\sum_k A_k \vec{I}_{k1} \right) \cdot \vec{S}. \quad (1)$$

These terms in order of relative strength are the Zeeman splitting, the hyperfine splitting due to the donor nucleus of spin I_D , and the hyperfine splitting due to the 4.7% abundant Si^{29} nuclei (located a distance $|\vec{r}_k|$ from the donor nucleus). When the site symmetry is T_d , a $1s (A_1)$ state has both g and A_D isotropic. The Fermi-Segré "contact" terms dominate the hyperfine interaction and

$$A_D = \frac{16}{3} \pi \mu_B (\mu_D / I_D) |\psi_D(0)|^2, \quad (2)$$

$$A_k = \frac{16}{3} \pi \mu_B (\mu / I) |\psi_D(\vec{r}_k)|^2,$$

where μ_B is the electronic Bohr magneton, μ_D and I_D are the magnetic moment and spin of the donor nucleus. The terms μ and I refer to the Si^{29} nuclei.

In the high-field limit, $g\mu_B H \gg A_D \gg A_k$ for all \vec{r}_k , and spin resonance occurs for the magnetic fields,

$$H_0 = \frac{1}{g\mu_B} \left(h\nu - A_D m_I - \sum_k A_k m_k \right). \quad (3)$$

Expression (3) describes the $(\text{Mg}^{25})^*$ spectrum of Fig. 1 with $(2I_D + 1) = 6$ lines of equal intensity spaced $(A_D / g\mu_B)$ apart, and centered about $g = 1.9981$. This g value describes the single line observed in the natural magnesium sample containing $(\text{Mg}^{24,26})^*$ donors for which $I_D = 0$. The P^{31} EPR lines from the simultaneously measured standard serve to calibrate the linear magnetic field sweep. Their separation is 42 G with their "center of gravity" at $g = 1.9985$. The measured $(\text{Mg}^{25})^*$ splitting is 30 G, from which we calculate

$$|\psi_D(0)|^2 = 2.0 \times 10^{24} \text{ cm}^{-3}$$

for $(\text{Mg}^+ : T_d)$. Identical spectra are obtained with $\vec{H} \parallel \langle 110 \rangle$. Therefore g and A_D are both isotropic, which is consistent with the optically assigned T_d site symmetry. A comparison of the $(\text{Mg}^+ : T_d)$ spin-Hamiltonian parameters with that of a sampling of other donors in Si is given in Table I. It is to be noted that both $|\psi_D(0)|^2$ and g of $(\text{Mg}^+ : T_d)$ are quite close to those of arsenic, although their optical binding energies are quite different.

Another feature of the $(\text{Mg}^+ : T_d)$ EPR absorption is that *only* six Mg^{25} hyperfine lines are observed, which is characteristic of an *isolated* Mg^+ donor. This observation excludes the association of Mg^+ ions. Clear EPR evidence for the association of an interstitial donor with itself or with compen-

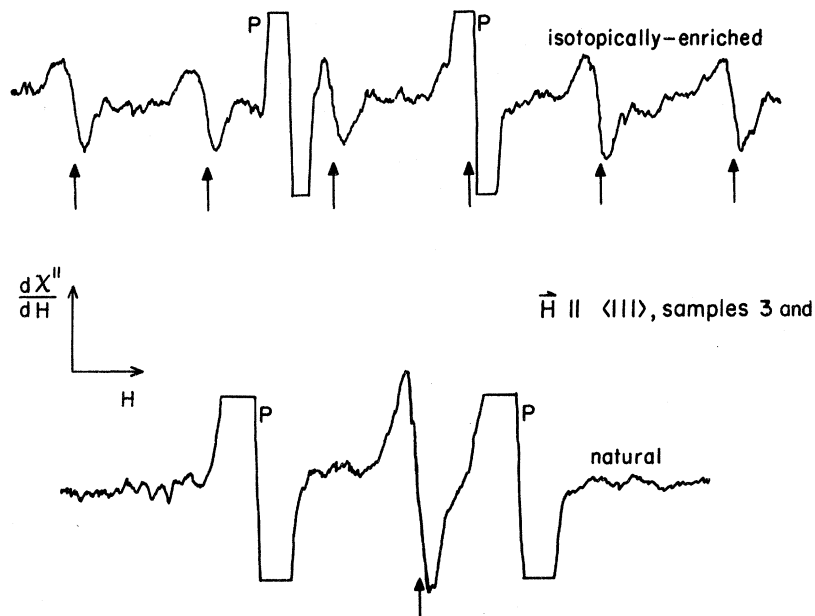


FIG. 1. Identification of the $(Mg^+ : T_d)$ spectrum by the use of a sample containing isotopically enriched Mg^{25} . The EPR absorption of $(Mg^{24})^+$ and $(Mg^{26})^+$ (natural magnesium) and $(Mg^{25})^+$ donors is denoted by arrows. The simultaneously measured phosphorus-doped standard, denoted by P, contained $\approx 10^{15} P^0/cm^3$. To minimize microwave saturation effects of $(Mg^+ : T_d)$, these measurements were made near $20^\circ K$ with a microwave power level of $\approx 0.2 \mu W$.

sating acceptors has been found in "slowly" cooled silicon doped with iron-group metals.⁹ Perhaps the most aesthetic example is the 21--hyperfine-line spectrum arising from a complex of four manganese donors.²¹ Even when a donor forms a complex with a zero-spin nucleus, such an association is observable by the induced anisotropic g value. An example is the Li-O complex.^{4,7} The absence of such distinctive effects argues for isolated Mg^+ donors.

The last term in Eq. (3) gives rise to the EPR linewidth; the Si^{29} interactions remain unresolved. The ENDOR technique of Feher⁴ has demonstrated that the group-V donors have "inhomogeneously" broadened EPR lines due to the "local" magnetic fields supplied by the Si^{29} nuclei. The EPR line shape is Gaussian to a good approximation since the number of contributing Si^{29} nuclei is large. The variation in the EPR linewidths among the group-V donors in Si and Ge can be reasonably accounted for by using the observed optical binding energies to correct the $1s(A_1)$ EMA wave functions.²² The EPR linewidth thus constitutes a check on the singlet wavefunction.

In our case, on account of the large samples (required because of the low Mg^+ densities), the EPR lines are artificially broadened by the magnetic-field gradient over the sample volume. The observed peak-to-peak linewidth has ranged from 3.5 to 4.3 G; both Mg^+ and P^0 give the same linewidth for a given run. Since the Si (Mg^+) samples are thicker than the Si (P) standard, we conclude that $\Delta H_{pp}(Mg^+) \lesssim \Delta H_{pp}(P) = 2.8 G$.⁴

The substitutional donor S^+ has a binding energy which is larger than that of Mg^+ . The hyperfine

interaction with some of the Si^{29} nuclei is sufficiently strong so that these "shells" (Si^{29} nuclei with the same $|\vec{r}_k|$) give a resolved splitting in the EPR spectrum. These additional splittings have been called "superhyperfine" (shf) lines to distinguish them from those of the donor nucleus. Superhyperfine transitions have also been observed in the EPR spectrum of Al^{3+} in silicon.²³ The shf lines can be used to distinguish the T_d substitutional lat-

TABLE I. EPR comparison of $(Mg^+ : T_d)$ with other donors studied in silicon.

Donor	G value ^a	$ \psi_D(0) ^2$ ($10^{24} cm^{-3}$)	Optical ^b binding energy (meV)
$(Mg^+ : T_d)$	1.9981	2.0	256.5 ^c
S^+	2.0054 ^d	34.0 ^d	520 ^d
Li-O	1.9978 (g_{II}) 1.9992 (g_I)	0.0033	39.4
P^0	1.9985	0.43	45.3
As^0	1.9984	1.70	53.5
Sb^0	1.9986	1.20	42.5
Bi^0	2.0003	14.0	70.5
EMA (delocalized donor EPR)	1.9988 ^a	0.08 ^e	30 ^f

^aReference 4.

^bReference 2.

^cReference 13.

^dReference 6.

^eW. Kohn and J. M. Luttinger, Phys. Rev. **97**, 883 (1955).

^fReference 1. Also see, R. A. Faulkner, Phys. Rev. **184**, 713 (1969). For Mg^+ and S^+ , the EMA value would be $\sim 4 \times 30 \approx 120$ MeV.

tice site from the T_d interstitial in the absence of ENDOR, although identifying these lines with particular Si²⁹ shells can be difficult.^{6,23} No shf lines have been observed in our experiments on Mg⁺. Their absence may arise because the charge concentration is insufficient at different Si lattice sites to give a resolved shf structure. This conclusion is uncertain because of the low Mg⁺ densities and the correspondingly low signal levels. Both S⁺ and Al³⁺ can be implanted in silicon to concentrations in excess of 10¹⁶ cm⁻³.

B. Effect of Light: The Metastable State (Mg⁺)^{*}

The (Mg⁺:T_d) spectrum undergoes a remarkable change with light, as shown in Fig. 2 for the natural magnesium samples. The single isotropic EPR line splits into two components with a 1:1 intensity ratio for $\vec{H} \parallel \langle 110 \rangle$ and a 3:1 ratio for $\vec{H} \parallel \langle 111 \rangle$. The improved signal-to-noise ratio of the light induced state (Mg⁺)^{*}, is the result of its sharply reduced spin-lattice relaxation time in comparison to (Mg⁺:T_d). The shorter T₁ values allow lower temperatures and higher microwave power levels to be used (viz., sample No. 2 of Fig. 2).

The measured *g* values of the component lines, and their relative intensities, reflect the $\langle 111 \rangle$ axial symmetry of the interstitial lattice site occupied by Mg⁺ when it is transformed into (Mg⁺)^{*}. The spectra of Fig. 2 can be described by

$$g^2(\theta) = g_{\parallel}^2 \cos^2 \theta + g_{\perp}^2 \sin^2 \theta, \quad (4)$$

where $g_{\parallel} = 1.9974$ and $g_{\perp} = 1.9986 (\pm 0.00015)$, and θ is the angle between \vec{H} and the $\langle 111 \rangle$ axis of the

Si unit cell. An identical symmetry has been found for the Li-O complex.⁴ Its $\langle 111 \rangle$ axis was explained as a displacement of the lithium atom from the T_d interstitial position (assigned to isolated lithium^{7,8}) caused by an interaction with a nearest-neighbor oxygen atom. A corresponding model for (Mg⁺)^{*} is not unreasonable. Such a model will be discussed in Sec. IV. It must, however, be shown that the light-induced spectra of Fig. 2 arises from magnesium donors. Light could for example transfer an electron from Mg⁺ to another impurity or lattice defect which then becomes paramagnetic. The exclusion of such a process is possible from the hyperfine "fingerprint" of (Mg²⁵)⁺ donors.

Figure 3 shows the effect of light on a Mg²⁵-enriched sample with $\vec{H} \parallel \langle 111 \rangle$. Rather than two lines with a 3:1 intensity ratio, the EPR spectrum with light is seen to be an overlap of at least seven lines. If the hyperfine splitting of (Mg²⁵)⁺ is isotropic (or unmeasurably anisotropic), each of the two lines with $\vec{H} \parallel \langle 111 \rangle$ would be expected to split into six components for a total of 12 lines. The 3:1 intensity ratio would be maintained for the two multiplets (each containing six equally spaced lines). The 12 lines of the spectrum with $\vec{H} \parallel \langle 110 \rangle$ would all have the same intensity. This anticipated spectrum is observed (Fig. 4). Although the derivative of the sum of 12 overlapping lines is difficult to visualize, the extremal lines marked A and B in Fig. 4 clearly exhibit the anticipated intensity ratios. The P⁰ standard was removed from the cavity to obtain Figs. 3 and 4 because the two P³¹ lines overlap the extreme lines of (Mg²⁵)⁺. The large overlap of the 12-line spectra is caused

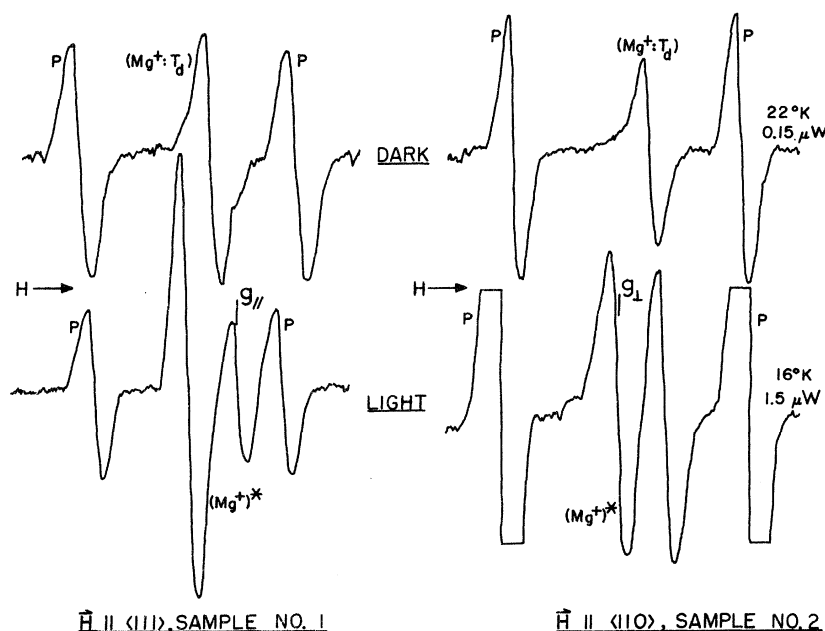


FIG. 2. Effect of light on the two natural magnesium samples. The (Mg⁺)^{*} *g* values are 1.9985 and 1.9974 for $\vec{H} \parallel \langle 111 \rangle$ and 1.9986 and 1.9978 for $\vec{H} \parallel \langle 110 \rangle$. The ratio of the Si(Mg⁺) to Si(P) standard-sample filling factors is 0.32/0.08 for sample No. 1 and 0.29/0.095 for sample No. 2.

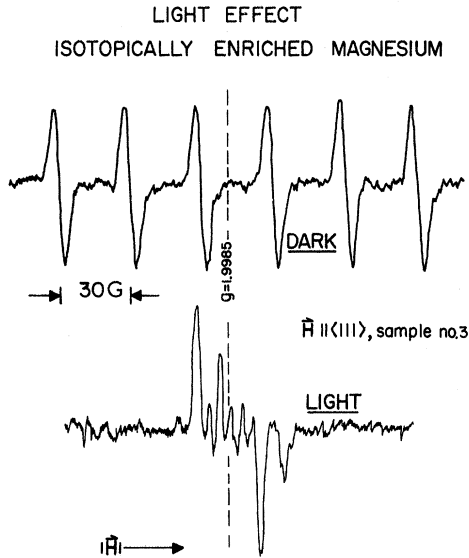


FIG. 3. Effect of light on a sample doped with Mg^{25} showing the "collapse" of the $(\text{Mg}^{25})^+$ hyperfine splitting. The magnetic field sweeping rates are equal with and without light. The respective temperature and power levels are different, having been selected for best signal-to-noise ratio.

by the fact that the hfs of $(\text{Mg}^+)^*$, 4.8 ± 0.2 G, is comparable with the individual linewidths (which are broadened by the inhomogeneous solenoid). From the $(\text{Mg}^{25})^*$ hfs we obtain

$$|\psi_D(0)|^2 = 0.33 \times 10^{24} \text{ cm}^{-3} \text{ for } (\text{Mg}^+)^*.$$

Near 4.2°K , the spin-lattice relaxation times for the group-V donors becomes quite long,²⁰ and EPR measurements can only be performed under various "passage" conditions.²⁴ Long spin-lattice relaxation times (i. e., $T_1 > 10^{-5}$ sec) are also observed for $(\text{Mg}^+ : T_d)$ up to at least 25°K . Because of the low Mg^+ concentrations, magnetic field modulation with phase-sensitive detection had to be used exclusively. At high enough temperatures and low enough microwave power levels, "slow passage" conditions could be obtained and T_1 measured by the same saturation method²⁵ used for the group-V donors²⁶ above 4.2°K , i. e., by measuring the absorptive component of the paramagnetic susceptibility as a function of microwave power.

In order to obtain T_1 by the saturation method²⁵⁻²⁷ we assumed that $T_1 = T_2$. The justification of this choice is based on the fact that in the range over which the measurements could be carried out $T_1 \ll T_2$ and the spin packets comprising the Mg^+ EPR line are " T_1 limited."²⁶ Gordon and Bowers²⁸ measured T_2 for P and Li donors in Si at 1.4°K as equal to 2.4×10^{-4} sec. The value of T_2 decreased to 2×10^{-4} sec for changes in the P concentration from 3×10^{16} to 10^{17} cm^{-3} ; it remained unchanged

when substitutional P donors were changed into interstitial Li donors. The value of T_2 doubled when P donors were studied in a crystal grown out of enriched Si^{28} . A similar estimate for the value of T_2 appears reasonable in the case of Mg^+ . This choice of T_2 leads to the conclusion that $T_1 \ll T_2$ for Mg^+ when $T \gg 9^\circ\text{K}$.

In reaching our estimates of T_1 we have not taken into account either the density gradient of the Mg^+ concentration in the sample or the variation of both the static and the rf magnetic fields over the volume of the sample. Both effects require appropriate averages²⁷ that are temperature independent and do not contribute to the temperature variation of T_1 . The latter is the significant result of Fig. 5. Castner's results for the shallow donors (dashed lines) are shown together with our results for Mg^+ , $(\text{Mg}^+)^*$, and P in Fig. 5.

Castner has shown²⁶ that at sufficiently high temperature T_1 is dominated by an Orbach²⁹ process,

$$(T_1)_{\text{Orbach}}^{-1} \propto e^{\Delta/k_B T}, \quad (5)$$

that arises because the spin relaxation of the $1s$ (A_1) state takes place through phonon-assisted transitions to higher lying $1s$ states, $1s(E)$ and $1s(T_2)$. The activation energy Δ is the energy difference between $1s(A_1)$ and $1s(T_2)$ or $1s(E)$. The Orbach-dominated temperature region for the

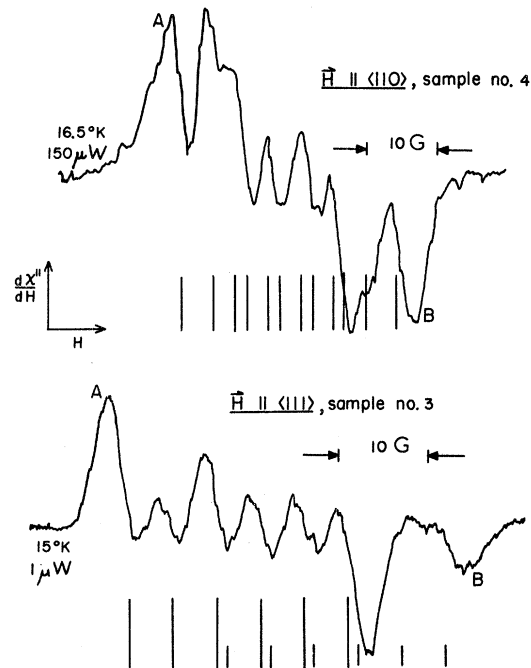


FIG. 4. Detailed sweeps of the $(\text{Mg}^{25})^+*$ spectra showing the positions of the component lines of the two six-line multiplets. With sample No. 4, each component line is equivalent to $\sim 8 \times 10^{12}$ spins/ cm^3 , or a total of $\sim 10^{11}$ spins.

group-V donors is given by dashed lines in Fig. 5. Castner's data have been used without correcting for a possible dependence of T_1 on the magnetic field.³⁰ The data of Ref. 26 were taken at 3.3 kG, while the present data were taken at 19.5 kG.

The slow variation of T_1 with temperature for $(Mg^+; T_d)$, i. e., the lack of an exponential dependence, is consistent with the large chemical shift established optically for this donor. Ho and Ramdas¹³ have been unable to observe optical transitions arising from either $1s(E)$ or $1s(T_2)$ when their samples were warmed to the vicinity of room temperature. If we make the reasonable assumption that these states lie near the EMA binding energy (as found for the group-V donors), then

$$\Delta \approx 255 - 120 \approx 135 \text{ meV.}$$

Since the largest phonon energy for silicon is ~ 60 meV,³¹ the description of T_1 by an Orbach process would not be expected to be valid for such a large chemical shift.

The temperature dependence of T_1 for $(Mg^+)^*$ differs substantially from that of $(Mg^+; T_d)$. The former is in fact very much like that of P^0 , which has a valley-orbit splitting ~ 10 meV. If the large change in T_1 when Mg^+ is optically excited is due

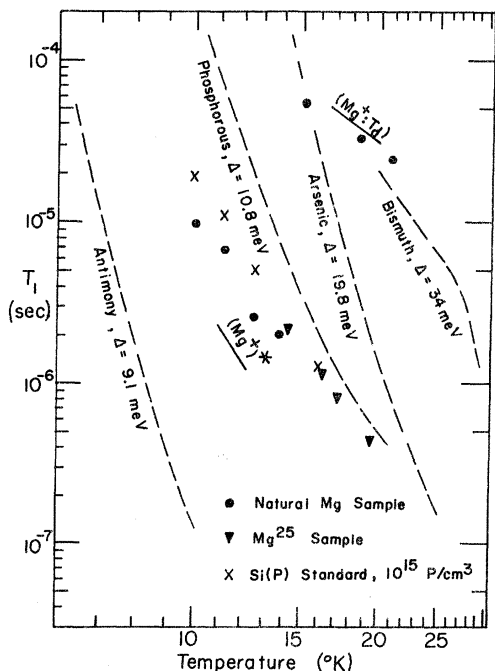


FIG. 5. Spin-lattice relaxation times as a function of temperature for two $Si(Mg^+)$ samples, together with the $Si(P)$ standard, determined from saturation plots. At 55 GHz, resonance occurs near 19500 G. The T_1 data for the group-V donors (dashed lines), and their respective Orbach-activation energies, have been taken from Ref. 26 (measured at 3300 G).

to the activation of an Orbach process, then the valley-orbit splitting of $(Mg^+)^*$ would be of the order of 10 meV. This value is very much smaller than that of the Mg^+ ion occupying the tetrahedral site.

C. $(Mg^+)^*$ Lifetime and Decay Characteristics

At sufficiently low temperature, the $(Mg^+)^*$ state remains sufficiently populated to be observed for minutes after the exciting light is turned off. We measured its decay by repeatedly sweeping through the EPR absorption in the dark. This method limits the lifetime measurement to times longer than ~ 10 sec. The low Mg^+ concentrations do not allow straight detection (time constant determined by the 30-GHz IF preamplifier) to be used.

The decay of the number of $(Mg^+)^*$ centers as a function of time, $n^*(t)$, is not exponential as would be expected for a monomolecular decay process (where all the Mg^+ ions decay independently to the ground state). The decay of $(Mg^+)^*$ back to $(Mg^+; T_d)$ can be well described by a bimolecular or two-body decay process where

$$dn^*/dt = -An^{*2}$$

and therefore,

$$n^*(t) = \frac{n^*(0)}{1 + An^*(0)t} \quad (6)$$

Thus a plot of $[n^*(0)/n^*(t) - 1]$ versus time should be linear, of slope $An^*(0)$. Such a linearity is demonstrated by Fig. 6. For the temperature range of Fig. 6, the light-on $(Mg^+)^*$ signal was the same at all temperatures (corrected for the $1/T$ dependence of the EPR signal), i. e., the optical conversion was complete. The relative slopes of Fig. 6 are then proportional to A only.

The decay data indicate that within experimental error, A is insensitive to temperature below $\sim 14^\circ K$. Below $10^\circ K$, the data are unreliable because of microwave saturation effects. The data of Fig. 6 are for those temperatures for which saturation effects could be avoided with good signal-to-noise ratio. Above $14^\circ K$, the value of A rapidly increases, with the $(Mg^+)^*$ lifetime decreasing from minutes to less than a second in the temperature interval of roughly $2^\circ K$. In this narrow temperature range, $A(T)$ can be fit to

$$A(T) = A_0 + A_1 e^{(-\theta'/T)}, \quad (7)$$

where A_0 is the average slope below $14^\circ K$. With obviously poor statistics, $\theta' \approx 50$ meV results from a fit to Eq. (7). Measuring this lifetime over a wider temperature interval would improve the value identified with either appropriate phonons or the ionization energy of the compensating boron acceptors.³² Another attractive possibility is that θ' corresponds to the binding energy of $(Mg^+)^*$, whose

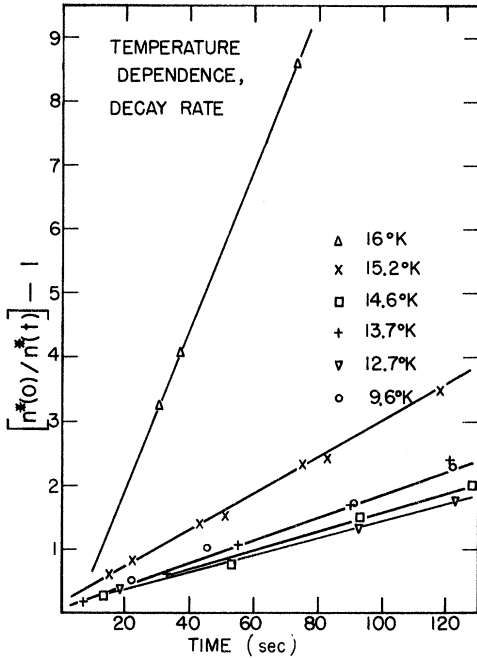


FIG. 6. Decay of the $(Mg^+)^*$ signal level $n^*(t)$ plotted to show the second-order decay kinetics. Below $\sim 10^\circ K$ light affects the value of T_1 , and such a measure of $n^*(t)$ is unreliable because of the very low microwave powers that must be used to avoid saturation.

value of $|\psi_D(0)|^2$ and whose temperature dependence of T_1 have been shown to be quite close to those of phosphorus (binding energy, 45 meV).

Above $16^\circ K$, it becomes increasingly difficult to populate $(Mg^+)^*$ with the ~ 5 mW of light available in the cavity. A study of n^* as a function of light intensity¹⁷ between 16 and $25^\circ K$ supports the second-order decay mechanism for $(Mg^+)^*$. Near $25^\circ K$, only $(Mg^+ : T_d)$ is observed.

The light quanta which convert the Mg^+ ions are *extrinsic*, i. e., the photoionization of Mg^+ takes place. Evidence for this conclusion is the following: (i) Placing silicon or germanium filters in the light path does not noticeably affect the bleaching of $(Mg^+ : T_d)$. The unfiltered light must also pass through up to 1.5 mm of silicon in the cavity to reach the Mg^+ -rich layer for a sample doped on only one side. (ii) At low temperatures the incandescent-lamp voltages used are less than 10% of maximum power, and thus the bulk of the light quanta are well below the Si absorption edge (1.16 eV at $4.2^\circ K$). (iii) A preliminary attempt by Ho and Ramdas³³ to bleach $(Mg^+ : T_d)$ with a He-Ne laser ($h\nu \approx 2$ eV) failed. (iv) If intrinsic quanta were important, one would expect either a bleaching or an enhancement of the Mg^+ EPR intensity instead of a photoconversion of Mg^+ . The capture of a photoelectron by Mg^+ would produce the nonparamagnetic state Mg^0 . An increase in the Mg^+ density would

instead result from the capture of an electron by Mg^{2+} ions. The photoholes would presumably be captured by the compensating boron acceptors. Neither of these possibilities is observed.

Intrinsic effects have been observed in other systems. In the case of *p*-type silicon in which electron-hole pairs are created by band light, the photoelectrons are captured by ionized compensating group-V donors and their EPR spectrum appears.³⁴ In the case of S^* in silicon, the creation of electron-hole pairs enhances the S^* spectrum⁶ by converting S^{2+} to S^+ . The S^{2+} is present because of the nonuniform sulfur doping.

IV. CONCLUSIONS: MODELS FOR PHOTOCONVERSION OF $(Mg^+ : T_d)$

The Mg^+ EPR data have shown that two distinct donor states are possible. In thermal equilibrium and in the dark, the Mg^+ ion occupies the T_d interstitial position. This state has previously been studied optically.¹⁰⁻¹³ Under illumination with near-infrared light, the equilibrium state at low temperatures is one where the Mg^+ ion occupies an interstitial site which has $\langle 111 \rangle$ axial symmetry. In the dark following illumination, the $(Mg^+)^*$ state decays to $(Mg^+ : T_d)$ with second-order kinetics. This decay rate rapidly increases above $14^\circ K$. We propose the following model, which although not unique, is attractive:

(i) The $(Mg^+ : T_d)$ ions are extrinsically photoionized to Mg^{2+} .
(ii) The resulting Mg^{2+} ions can occupy *either* the T_d or another interstitial site located along $\langle 111 \rangle$, possibly the C_{3v} hexagonal position. Weiser³⁵ has shown that the occupation probability of an impurity at either the T_d or C_{3v} interstitial site depends strongly on its size. The latter site has an available volume only slightly smaller than the former. Weiser calculated the occupation probability of lithium, by using an attractive potential due to the polarization induced in the neighboring Si atoms and a repulsive potential arising from the overlap of Li and Si core electrons. Contrary to what has since been observed experimentally^{7,8} for Li^0 , Weiser predicted C_{3v} to be the preferred position. None of the interstitial donors studied in silicon has been found to prefer the C_{3v} site. We speculate that Mg^{2+} has a "critical" ionic radius such that once formed, it can occupy either interstitial site.

(iii) The Mg^{2+} ions are distributed between the T_d and C_{3v} lattice sites during illumination. The photoionized electrons can be recaptured at either $(Mg^{2+} : T_d)$ or $(Mg^{2+} : C_{3v})$. Mg^+ formed at the latter site is $(Mg^+)^*$, which is shallow in comparison to the reformed $(Mg^+ : T_d)$. The shallow nature of $(Mg^+)^*$ is supported by its phosphoruslike EPR description. With extrinsic quanta limited to the

range $0.5 \lesssim h\nu \lesssim 1.2$ eV by the quartz light pipe and the silicon filter, $(\text{Mg}^+)^*$ will be much less effectively photoionized than $(\text{Mg}^+ : T_d)$ since the extrinsic photoionization cross section is a rapidly decreasing function of the photon energy above the threshold.³⁶ Thus, at low temperatures under illumination, the $(\text{Mg}^+)^*$ state is long lived in comparison to $(\text{Mg}^+ : T_d)$ and the photoconversion is complete.

(iv) During illumination and immediately after the light is turned off, $(\text{Mg}^+ : T_d)$ has been converted to $(\text{Mg}^+)^*$. The long lifetime of $(\text{Mg}^+)^*$ in the dark implies that the potential barrier separating the two sites is large and the recovery of $(\text{Mg}^+ : T_d)$ by tunneling is improbable. Because of the fact that the $(\text{Mg}^+)^*$ decay is *not* monomolecular, we conclude that tunneling is not an important process for $T \geq 10^\circ\text{K}$. Since $(\text{Mg}^+)^*$ is shallow it may be thermally ionized; at a given time there will be n free electrons and an equal number of Mg^{++} ions, which on the basis of step (ii) redistribute themselves among the T_d and C_{3v} sites. The probability of recapture by the Mg^{++} ions would then be proportional to n^2 , satisfying the bimolecular decay kinetics observed for $(\text{Mg}^+)^*$. The reformation of $(\text{Mg}^+ : T_d)$ would be permanent in the dark since this state is deep. In this model, the activation energy θ' of Eq. (7) would correspond to the binding energy of $(\text{Mg}^+)^*$. The 50 MeV assignment of θ' is consistent with the phosphoruslike value of $|\psi_D(0)|^2$ for $(\text{Mg}^+)^*$. The insensitivity to temperature below 14°K of the $(\text{Mg}^+)^*$ lifetime may be due to the increasing importance of a competing process. Monomolecular decay kinetics to be expected for a tunneling process cannot be checked with the present experiments because of microwave saturation effects below 10°K .

All of the EPR data on $(\text{Mg}^+)^*$ can be explained by an ionic-motion model, although not in a unique way. There is another possibility that arises on account of the inhomogeneous Mg^+ distribution. Since the effective Mg^+ density is nearly an order of magnitude lower than the compensating boron density, the presence of Mg^{++} in the interior portion of our samples is certain; the Mg^+ valence state is confined to near the surface. These Mg^{++} ions, present in thermal equilibrium and in the dark,

could provide a different mechanism for the photoconversion of Mg^+ . In this model, the $\langle 111 \rangle$ axial symmetry would not arise from a *motion* of the isolated Mg^{++} ions created by light, but rather from an *association* of the original Mg^{++} ions with another defect. A capture by these Mg^{++} ions of the electrons ionized from Mg^+ would satisfy all of the EPR evidence obtained for $(\text{Mg}^+)^*$. Just as in the case of the ionic-motion model, the recovery of $(\text{Mg}^+ : T_d)$ would have to proceed by thermal ionization to explain the second-order kinetics. No additional hyperfine lines have been observed with $(\text{Mg}^+)^*$. Such spectral features would identify the associating defect. The absence of additional hfs could be explained by either a small value of $|\psi_D(\vec{r}_k)|^2$ at the substitutional site occupied by the defect, or by the defect having a zero nuclear spin, as for example Mg^{++} associated with either oxygen³⁷ or a lattice vacancy.

Since $(\text{Mg}^+ : T_d)$ and Mg^{++} occupy different portions of the samples, the creation of $(\text{Mg}^+)^*$ would proceed by the diffusion of the electrons photoionized from $(\text{Mg}^+ : T_d)$, into the Mg^{++} -rich region. Because of space-charge effects, the buildup of $(\text{Mg}^+)^*$ would be slow in comparison to the ionic motion mechanism.

Both of these mechanisms may coexist. In order to gauge their relative importance, it would be interesting to study the $(\text{Mg}^+)^*$ formation kinetics with an applied electric field. If the association mechanism is dominant, the creation and decay time of $(\text{Mg}^+)^*$ would be expected to be a strong function of the electric field strength and polarity. An equally important experiment would be the study of $(\text{Mg}^+)^*$ optically to determine its binding energy. If the conclusions reached from the EPR data are correct, its binding energy should be close to 50 meV, i. e., near that of the group-V donors.

ACKNOWLEDGMENTS

The authors are grateful to Professor A. K. Ramdas for suggesting the study of the Mg^+ donor in Si as well as for a critical reading of the manuscript. They are grateful to Professor A. K. Ramdas and Dr. L. T. Ho for keeping them informed on their work prior to publication.

*Work supported in part by the National Science Foundation under Grant No. GP-7021.

¹W. Kohn, in *Solid State Physics*, edited by F. Seitz and D. Turnbull (Academic, New York, 1957), Vol. 5, p. 259.

²Fisher and A. K. Ramdas, in *Physics of the Solid State*, edited by S. Balakrishna (Academic, New York, 1969).

³G. Dresselhaus, A. F. Kip, and C. Kittel, *Phys. Rev.* **98**, 368 (1955).

⁴G. Feher, *Phys. Rev.* **114**, 1219 (1959).

⁵W. E. Krag and H. J. Zeiger, *Phys. Rev. Lett.* **8**, 485 (1962); W. E. Krag, W. H. Kleiner, H. J. Zeiger, and S. Fischler, *J. Phys. Soc. Jap. Suppl.* **21**, 230 (1966).

⁶G. W. Ludwig, *Phys. Rev.* **137**, 739 (1964).

⁷R. L. Aggarwal, P. Fisher, V. Mourzine, and A. K. Ramdas, *Phys. Rev.* **138**, A882 (1965).

⁸G. D. Watkins and F. S. Ham, *Phys. Rev. B* **1**, 4071 (1970).

⁹G. W. Ludwig and H. H. Woodbury, in *Solid State Physics*, edited by F. Seitz and D. Turnbull (Academic, New York, 1962), Vol. 13, p. 223.

¹⁰R. K. Franks and J. B. Robertson, *Solid State Commun.* **5**, 479 (1967).

¹¹L. T. Ho and A. K. Ramdas, *Phys. Lett.* **32**, 23 (1970); *Phys. Rev. B* **5**, 462 (1972).

¹²R. K. Franks and J. B. Robertson, *Solid State Commun.*

6, 825 (1968); R. K. Crouch, J. B. Robertson, and T. E. Gilmer, Phys. Rev. B **5**, 3111 (1972).

¹³L. T. Ho, Ph.D. thesis (Purdue University, 1971) (unpublished).

¹⁴E. B. Hale and R. L. Miehler, Phys. Rev. **184**, 739 (1969).

¹⁵Obtained from Dow Chemical Co., Midland, Mich. This material contained a maximum of 0.002% by weight of any metallic contaminant.

¹⁶Obtained from the Isotope Sales Dept., Oak Ridge National Laboratory: 99.21% Mg²⁵, 0.39% Mg²⁴, and 0.40% Mg²⁶. All other metallic nuclei $\lesssim .05\%$ by weight.

¹⁷J. E. Baxter, Ph.D. thesis (Purdue University, 1972) (unpublished).

¹⁸G. Feher, J. C. Hensel, and E. A. Gere, Phys. Rev. Lett. **5**, 309 (1960).

¹⁹J. C. Hensel, Phys. Rev. **138**, A225 (1965).

²⁰G. Feher and E. A. Gere, Phys. Rev. **114**, 1245 (1959).

²¹G. W. Ludwig, H. H. Woodbury, and R. O. Carlson, Phys. Chem. Solids **8**, 490 (1959).

²²D. K. Wilson, Phys. Rev. **134**, A265 (1964).

²³K. L. Brower, Phys. Rev. B **1**, 1908 (1970).

²⁴M. Weger, Bell Syst. Tech. J. **39**, 1013 (1960).

²⁵A. M. Portis, Phys. Rev. **91**, 1071 (1953).

²⁶T. G. Castner, Phys. Rev. Lett. **8**, 13 (1962); Phys. Rev. **130**, 58 (1963).

²⁷T. G. Castner, Phys. Rev. **115**, 1506 (1959).

²⁸J. P. Gordon and K. D. Bowers, Phys. Rev. Lett. **1**, 368 (1958).

²⁹C. B. P. Finn, R. Orbach, and W. P. Wolf, Proc. R. Soc. Lond. **77**, 261 (1961).

³⁰T. G. Castner, Phys. Rev. **155**, 816 (1967).

³¹B. N. Brockhouse, Phys. Rev. Lett. **2**, 256 (1959).

³²A. Onton, P. Fisher, and A. K. Ramdas, Phys. Rev. **163**, 686 (1967).

³³L. T. Ho and A. K. Ramdas (private communication).

³⁴G. Bemski and B. Szymanski, J. Phys. Chem. Solids **17**, 173 (1960).

³⁵K. Weiser, Phys. Rev. **126**, 1427 (1962).

³⁶H. A. Bethe and E. E. Salpeter, *Quantum Mechanics of One and Two Electron Atoms* (Academic, New York, 1957), p. 300.

³⁷We have used floating zone-refined silicon to prepare our samples. The presence of oxygen cannot be entirely excluded since during diffusion of the magnesium the oven tubes were open at one end with helium gas continuously flushed through the inner tube containing the sample.

Numerical Study of Two-Phonon Sidebands in the Optical Absorption of Free Polarons in the Strong-Coupling Limit*

M. J. Goovaerts, J. M. De Sitter, and J. T. Devreese^{†‡}
Institute for Applied Mathematics, Faculty of Sciences, State University of Antwerp,
Middelheimlaan 1, Antwerp, Belgium
 (Received 23 March 1972)

Using the theory and the analytical results of Kartheuser, Evrard, and Devreese (KED), we have calculated numerically the two-phonon sideband in the optical absorption coefficient of free polarons. Therefore, integrals of the type

$$\int \int \int (d\vec{k}/k^2) \int \int (d\vec{k}'/k'^2) \vec{k} \cdot \vec{k}'^{2j} \cos^{2j} \theta' k^{2i} \cos^{2i} \theta \delta((\vec{k} + \vec{k}')^2 - \epsilon^2) e^{-x\vec{k}^2 - y\vec{k}'^2},$$

as obtained by KED, are treated analytically and reduced to a finite sum of single integrals for integer i and $j > 0$, for all real $x, y > 0$ and for any real ϵ . Our numerical results, combined with the zero-phonon line and the one-phonon sideband obtained by KED, confirm the mechanism for the absorption of light by free polarons proposed by KED.

I. INTRODUCTION

Kartheuser, Evrard, and Devreese¹ (KED) treated the optical absorption coefficient of free Fröhlich polarons in the Landau-Pekar approximation, which is essentially valid for strong coupling.

The physical picture emerging from Ref. 1 is the following: At strong coupling there is an intense sharp peak in the optical absorption due to a transition from the polaron ground state to the first relaxed excited polaron state (RES). This zero-phonon peak is accompanied by *sidebands* due to the emission of 1, 2, 3, ..., n , ... free phonons along with the absorption process.

KED gave the general expressions for the absorption coefficient in the Landau-Pekar approxi-

mation and calculated explicitly the one-phonon sideband, the low-frequency part of the two-phonon sideband, and the zero-phonon peak in the one-phonon approximation.^{1,2}

The purpose of KED's work was to show the role of relaxed excited polaron states in the optical absorption process.³ Until now no numerical calculation of the complete *two-phonon sideband* has been published. It is the purpose of the present paper to provide such a calculation using the expressions derived by KED.

Our calculation not only adds information about the polaron absorption spectrum; it also contributes to clarify the problem, especially in the coupling region where one- and two-phonon processes occur while processes with three and more phonons are unimportant ($5 \lesssim \alpha \lesssim 7$). Furthermore, it gives